BIOLOGY OF REPRODUCTION **82,** 617–627 (2010)
Published online before print 9 December 2009.
DOI 10.1095/biolreprod.109.080408

Development and Characterization of a Three-Dimensional Organotypic Human Vaginal Epithelial Cell Model[1]

Brooke E. Hjelm,[3,4,5] Alice N. Berta,[3] Cheryl A. Nickerson,[3,4] Charles J. Arntzen,[3,4] and Melissa M. Herbst-Kralovetz[2,3,6]

Center for Infectious Diseases and Vaccinology,[3] The Biodesign Institute at Arizona State University, Tempe, Arizona
School of Life Sciences,[4] Arizona State University, Tempe, Arizona
Neurogenomics Division,[5] The Translational Genomics Research Institute, Phoenix, Arizona
Department of Basic Medical Sciences,[6] University of Arizona College of Medicine-Phoenix in partnership with Arizona State University, Phoenix, Arizona

ABSTRACT

We have developed an in vitro human vaginal epithelial cell (EC) model using the innovative rotating wall vessel (RWV) bioreactor technology that recapitulates in vivo structural and functional properties, including a stratified squamous epithelium with microvilli, tight junctions, microfolds, and mucus. This three-dimensional (3-D) vaginal model provides a platform for high-throughput toxicity testing of candidate microbicides targeted to combat sexually transmitted infections, effectively complementing and extending existing testing systems such as surgical explants or animal models. Vaginal ECs were grown on porous, collagen-coated microcarrier beads in a rotating, low fluid-shear environment; use of RWV bioreactor technology generated 3-D vaginal EC aggregates. Immunofluorescence and scanning and transmission electron microscopy confirmed differentiation and polarization of the 3-D EC aggregates among multiple cell layers and identified ultrastructural features important for nutrient absorption, cell-cell interactions, and pathogen defense. After treatment with a variety of toll-like receptor (TLR) agonists, cytokine production was quantified by cytometric bead array, confirming that TLRs 2, 3, 5, and 6 were expressed and functional. The 3-D vaginal aggregates were more resistant to nonoxynol-9 (N-9), a contraceptive and previous microbicide candidate, when compared to two-dimensional monolayers of the same cell line. A dose-dependent production of tumor necrosis factor-related apoptosis-inducing ligand and interleukin-1 receptor antagonist, biomarkers of cervicovaginal inflammation, correlated to microbicide toxicity in the 3-D model following N-9 treatment. These results indicate that this 3-D vaginal model could be used as a complementary tool for screening microbicide compounds for safety and efficacy, thus improving success in clinical trials.

3-D organotypic model, cytokines, female reproductive tract, immunology, innate immunology, pathogen-associated molecular patterns (PAMPs), rotating wall vessel (RWV) bioreactor, toll-like receptors (TLRs), vagina, vaginal microbicide screening

INTRODUCTION

Vaginal epithelial cells (ECs) provide the first line of defense for women exposed to sexually transmitted infections (STI) [1, 2]. These cells can provide both structural and immunological defense mechanisms against STI pathogens. In vivo, vaginal ECs are characterized as sheets of multicellular stratified squamous epithelia that exhibit tissue-specific protein expression patterns between the basal and suprabasal surfaces, produce mucus glycoproteins that aid in enzymatic and pathological defense, and exhibit distinct morphological features like microfolds, microridges, and cell-cell adhesion structures [3–7]. These ECs also play a critical role in immunological response to pathogens and pathogen-associated molecular patterns (PAMPs) through toll-like receptor (TLR) signaling cascades, cytokine and chemokine production, as well as immune cell recruitment and activation [1, 2, 8, 9]. All of these features are physiologically relevant attributes of vaginal ECs that should be present in an organotypic vaginal EC model developed for microbicide and/or STI research.

Microbicides are agents that can be applied topically to the vagina or rectum and provide a promising approach for STI prevention. These compounds can act directly on the STI pathogen, or they can act indirectly by inducing innate immune responses in the genital epithelia and/or by recruiting immune cells to the site of infection. In addition to the direct or indirect mechanisms of action that a particular microbicide may exhibit, it is equally crucial that the compound does not cause uncontrolled inflammation, toxicity, or damage to the integrity of the vaginal epithelia [10–12].

Nonoxynol-9 (N-9) is the active ingredient in the over-the-counter spermicide Conceptrol, and it has gained particular attention after it showed anti-HIV activity both in vitro and in animal models. Unfortunately, this compound subsequently failed clinical trials and, in some cases, increased the incidence of HIV transmission [13, 14]. It has been hypothesized that increased HIV transmission after N-9 treatment was caused by the disruption of the mucosal epithelial barrier and integrity, recruitment of HIV-susceptible immune cells, genital EC inflammation, and/or microbicide-induced changes in the natural vaginal flora [12–14]. Because N-9 was shown to disrupt the human vaginal EC barrier and has been studied in humans in vivo, it has become an excellent tool for validating cell culture, tissue explants, and animal models for their relevance as microbicide safety and efficacy models [13, 15].

Several studies have indicated that various primary and immortalized cell lines grown as traditional monolayers on impermeable plastic surfaces or suspension cultures are significantly more susceptible to N-9 toxicity than surgical

[1]Supported by a grant from the Sexually Transmitted Infections and Topical Microbicides Cooperative Research Center (1 U19 AI062150-01).
[2]Correspondence: Melissa M. Herbst-Kralovetz, Center for Infectious Diseases and Vaccinology, The Biodesign Institute at Arizona State University, 1001 South McAllister Avenue, Tempe, AZ 85287-5401. FAX: 480 727 7615; e-mail: melissa.herbst-kralovetz@asu.edu

Received: 23 July 2009.
First decision: 2 September 2009.
Accepted: 17 November 2009.

eISSN: 1529-7268 http://www.biolreprod.org
ISSN: 0006-3363

explants and various animal models, which more closely mimic the physiological features of human reproductive tract tissues [12, 16, 17]. As such, human and animal explants from vaginal and cervical biopsies have become a primary in vitro method for microbicide evaluation [11, 18]. Several caveats of these explant models have been described and include a progressive deterioration of tissue architecture in explanted tissues as well as limitations with tissue availability, variability between samples, and the requirement for Institutional Review Board approval [11, 17]. While these explant models do provide a powerful tool for evaluating microbicide safety and efficacy in the female reproductive tract, they are not an ideal model for high-throughput evaluations.

High-throughput screening provides the means to test cellular viability in response to a greater number of compounds simultaneously in addition to evaluating signature biomarkers, which have become increasingly important molecules for diagnosing cervicovaginal inflammation. There have been a number of biomarkers implicated in cervicovaginal inflammation. Among these biomarkers, we evaluated the endogenous antagonist of interleukin-1 (IL1RN or IL-1RA), tumor necrosis factor-related apoptosis-inducing ligand (TRAIL), interferon gamma (IFNG), interleukin 6 (IL6), IL8 (or CXCL8), regulated upon activation, normal T-cell expressed and secreted (RANTES, official symbol CCL5), and interferon-inducible protein 10 (IP-10, official symbol CXCL10) [2, 8, 11, 19–21]. Cytokine-signaling cascades can contribute to proinflammatory and anti-inflammatory immune responses as well as immune cell recruitment and activation. These biomarkers have provided valuable screening tools for microbicide studies and are particularly well suited for high-throughput in vitro evaluations.

Several of these cytokines can be triggered by TLR activation from microbial ligands or synthetic TLR agonists. These TLRs can play an integral role in sensing both pathogens and some microbicide compounds, and have been implicated as key players in mucosal homeostasis [1, 10, 22]. TLR2, 3, 5, and 6 have been shown to be highly expressed and functionally bioactive in vaginal ECs [1, 23–25]. Therefore, candidate microbicide screening should include analysis of TLR-mediated cytokine production, especially since a recent report by Trifonova et al. [10] demonstrated that a class of microbicides could inhibit TLR responsiveness in genital epithelia.

In addition to the in vitro methods available for microbicide evaluation, animal models play an integral role in the microbicide development pipeline. The standardized model for vaginal toxicity studies is the rabbit vaginal irritation model; however, additional microbicide evaluation studies have been conducted in mouse and macaque animal models [12, 26–28]. While these animal models provide valuable tools for evaluating the histopathological, systemic, and immunological effects of microbicides, they may not accurately predict human toxicity due to species variations and are not ideal platforms for high-throughput toxicity testing.

Our collaborative group has utilized the rotating wall vessel (RWV) bioreactor technology to create several three-dimensional (3-D) cell culture models (i.e., gastrointestinal, lung, colon, placental, and neuronal) that exhibit physiologically relevant features observed in vivo [29–33]. This technology has produced 3-D models, grown in a physiological, low fluid shear environment, that have been shown to mimic key aspects of the parental tissue in vivo and that have been applied to study bacterial and viral pathogenesis, tumorogenesis, osteogenesis, hormone and protein expression, etc. [34–37]. The RWV bioreactor technology exposes cell cultures to gravitational, centrifugal, and Coriolis forces, causing a gradual sedimentation of the cells as the vessel turns; this controlled rotation minimizes detrimental shear forces and allows the cells to form 3-D, tissue-like aggregates [38, 39]. To our knowledge, this is the first report to exploit the RWV technology to develop and characterize a 3-D organotypic vaginal EC model for high-throughput analysis of candidate microbicides and STI pathogenesis research specific to the vaginal EC microenvironment. Overall, this in vitro model preserves the functional architecture of the parental vaginal tissue, yet retains the ease and accessibility of an immortalized vaginal EC line.

MATERIALS AND METHODS

Mammalian Cell Culture

Vaginal EC monolayers. The immortalized vaginal EC (V19I) line was kindly provided by Dr. Richard Pyles, and cells were cultured as previously described [1, 25, 40]. V19I monolayers were grown in T-150 flasks (BD Falcon; BD Biosciences, San Jose, CA), released with 0.25% trypsin (Mediatech, Inc., Manassas, VA), and enumerated as previously described [1]. Cell quantification was performed either manually with a hemacytometer or automatically with the Countess automated cell counter (Invitrogen, Carlsbad, CA). Confluent vaginal EC monolayers (passages 8–18) were used for all the experiments.

Three-dimensional vaginal EC model. V19I cell suspensions (3×10^6 cells) were mixed with 0.3 grams of type 1 collagen-coated dextran microcarrier beads (Cytodex-3; Sigma-Aldrich, St. Louis, MO). Microcarrier beads were autoclaved in sterile Dulbecco PBS (DPBS) (Invitrogen) (110°C, 20 min) and were allowed to swell at ambient temperature for at least 3 days before being combined with the V19I cell suspensions. Cells/beads were seeded (Day 0) in 55 ml of media in the rotating wall vessel (RWV; Synthecon, Inc., Houston, TX), which was allowed to incubate prior to rotation for 0.5 h at 37°C and 5% CO_2 and was subsequently cultured at a rate of approximately 20 rotations per min. Images and technical descriptions of RWV bioreactors have been reviewed by Navran [39]. Culture media was changed 96 h after the RWV was seeded, every 48 h until Day 12, and then every 24 h until the aggregates were ready to harvest (Days 39–42). In addition to changing the media, an additional 1×10^6 V19I cells were added to the rotating culture once an initial layer of cells had grown on the beads (~Day 21) to ensure a more uniform culture. Samples of the 3-D vaginal aggregates (500 µl) were monitored frequently by differential interference contrast (data not shown), confocal, and electron microscopy analyses. After 39–42 days rotating in the RWV culture, all of the 3-D cell aggregates were harvested and either fixed for morphological and histological analysis, or plated in a 24-well plate for cell treatments/stimulation experiments. A single RWV (55-ml volume) consistently yielded two 24-well plates with at least 2×10^4 cells/well. Prior to use in all the assays, cell viability was determined using trypan blue.

Electron Microscopy

Primary fixation. The 3-D vaginal aggregates were fixed in fresh, primary fixative (2% glutaraldehyde/2% formaldehyde (Electron Microscopy Sciences, Hatfield, PA) in DPBS for 0.5 h at ambient temperature and were incubated in the primary fixative for an additional 24 h at 4°C. The fixative was removed, and the aggregates were washed three times in DPBS. Aggregates were then fixed/stained in 1% osmium tetroxide (OsO_4) (Electron Microscopy Sciences) in double-distilled H_2O (ddH_2O) for 1 h at ambient temperature. The aggregates were then washed three times in ddH_2O. All subsequent fixation and staining procedures described were performed at ambient temperature.

Transmission electron microscopy secondary fixation, sample preparation, and microscopy. For transmission electron microscopy (TEM) studies, aggregates were then stained en bloc with 1% uranyl acetate (Electron Microscopy Sciences) in ddH_2O for 1 h. The aggregates were washed again three times in ddH_2O. Samples were then dehydrated in a seven-step series of ethanol solutions, followed by a 10-min equilibration in 1:1 ethanol:acetone. The aggregates were then stained en bloc with 1% (saturated) lead acetate (Malliinckrodt Baker, Phillipsburg, NJ) diluted in the ethanol/acetone solution for an additional 1 h. The aggregates were then rinsed twice in the ethanol/acetone solution, followed by two dehydration steps in 100% acetone. The acetone was removed, and the aggregates were placed in a progression of Spurr's resin (Electron Microscopy Sciences)/acetone solutions, during which time the resin concentration was increased every 12 h. Aggregates were then removed from the glass jars and placed into vertical conical molds in 100% Spurr's resin that was allowed to polymerize in a 60°C oven for 24 h. Once the

blocks containing cells of interest were identified, ultrathin sections (80 nm) were cut with a diamond knife (Diatome, Hatfield, PA) on a Leica Ultracut R microtome and were placed on formvar-coated 200-mesh copper grids (Electron Microscopy Sciences). Samples were imaged with a Philips CM12 Transmission Electron Microscope, and images were acquired using a Gatan 791 CCD camera and software (Gatan, Pleasanton, CA).

Scanning electron microscopy sample preparation and microscopy. For scanning electron microscopy (SEM) studies, aggregates were dehydrated in a series of acetone solutions, dried with a CPD020 critical point dryer (Balzers, Wiesbaden, Germany), and sputter-coated for 7 min with platinum in a Technics Hummer II sputter coater (Technics, Alexandria, VA). Samples were imaged with a Leica Cambridge Stereoscan 360 FE scanning electron microscope (Leica Cambridge Co., Cambridge, U.K.) using the EDS 2006 software (IXRF Systems Inc., Houston, TX).

Immunofluorescence

Sample preparation and microscopy. The 3-D vaginal EC aggregates, or monolayers grown on coverslips (Fisher Scientific, Pittsburg, PA), were fixed for 0.5 h at ambient temperature in 4% formaldehyde (Electron Microscopy Sciences) and then washed three times in DPBS. Cells were permeabilized in 0.5% Triton X-100 (Electron Microscopy Sciences) in DPBS for 5 min. The 3-D vaginal EC aggregates were blocked in 8% BSA (Sigma-Aldrich) in DPBS for 1 h at 37°C. The two-dimensional (2-D) vaginal EC monolayers were blocked in 8% BSA in DPBS for 0.5 h at ambient temperature in a humidifying chamber. Samples were then incubated 2 h at 37°C or overnight at 4°C with the following primary antibodies: MUC1 (1:50; Santa Cruz Biotechnology, Santa Cruz, CA), MUC4 (1:10; Zymed Laboratories, San Francisco, CA), MUC5AC (1:50; Zymed Laboratories), ZO-1 (1:100; Zymed Laboratories), E-cadherin (1:50; Chemicon, Billerica, MA), ESA (1:50; Chemicon), CD1D (1:200; Abcam, Cambridge, MA), and involucrin (1:250; Sigma-Aldrich). Cells were then washed with 0.1% Tween 20 (VWR, West Chester, PA) in PBS (T-PBS), incubated for 1 h with the appropriate fluorophore-conjugated secondary antibody diluted 1:250 to 1:500 (Alexa Fluor 555; Invitrogen), washed again in T-PBS, rinsed once in water, and mounted in ProLong Gold antifade reagent with 4′,6-diamidino-2-phenylindole (Molecular Probes, Invitrogen). Optical sections (1–2 μm) through the z-plane of the cell layers were obtained using a Zeiss LSM 5 DUO laser scanning confocal microscope and analyzed using the Zeiss LSM browser software package (Carl Zeiss, Thornwood, NY). Z-Stack images were reconstructed from fifty to one hundred 1–2 μm optical sections using the Zeiss LSM software package (Carl Zeiss). All immunofluorescence results were verified in multiple batches of 3-D vaginal EC aggregates.

Nonoxynol-9 Treatment and Cell Viability Assay

Cell treatment procedure. Three-dimensional vaginal EC model aggregates were removed from the RWV bioreactors and distributed evenly in 24-well tissue culture plates (BD Falcon; BD Biosciences) for testing at a density of at 2×10^4 cells/well. Monolayers were seeded into separate 24-well plates at the same density. Two wells of each plate were trypsinized (0.25%; Mediatech, Inc.) and enumerated by trypan blue (Mediatech, Inc.) exclusion to determine initial cell viability/concentration. Nonoxynol-9 (Ortho Options Conceptrol; McNeil-PPC, Inc., Fort Washington, PA) was added to duplicate wells at 20, 100, and 500 μg/ml, all diluted in sterile DPBS. In addition, sterile DPBS treatments were performed and used as a negative control. All the structural and functional characterization was performed within 48 h after removal from the RWV; however, aggregates retain structural morphology and viability for at least 72 h postplating.

Cell viability assay. Cell supernatants (120 μl) were collected from each well at 1.5, 4, 8, and 24 h, and analyzed by cytometric bead array (CBA) (Bio-Plex; Bio-Rad, Hercules, CA) for cytokine/chemokine production. In addition, DPBS- and N-9-treated wells were harvested, trypsinized, and enumerated by trypan blue (Mediatech, Inc.) exclusion to determine the cell viability for each time point.

TLR Agonist Treatments and Cytokine Quantification

TLR agonists. The 3-D vaginal EC aggregates or monolayers were plated at 2×10^4 cells/well in 24-well tissue culture treated plates (BD Falcon; BD Biosciences). TLR agonists were added to vaginal ECs at the following concentrations: FSL-1 (InvivoGen, San Diego, CA), a synthetic lipoprotein derived from *Mycoplasma salivarium* and a TLR2/6 heterodimer agonist (0.1 μg/ml); polyinosinic:polycytidylic acid (PIC) (InvivoGen), a synthetic form of double-stranded RNA and a TLR3 agonist (100 μg/ml); flagellin (FLAG) (InvivoGen), the major component of bacterial flagellar filaments and a TLR5 agonist (5 μg/ml); CL097 (InvivoGen), an imidazoquinoline compound with potent antiviral activity and a TLR7/8 agonist (10 μg/ml); and sterile DPBS. Cell supernatants (120 μl) were collected from each well at 24 h poststimulation and were frozen at −20°C until analysis by CBA to determine TLR activity (i.e., cytokine/chemokine production).

Cytokine/chemokine quantification. Cytokine analysis was determined by CBA. A custom human CBA kit was constructed that contained the following targets: TRAIL, IL1RN, IL6, IL8, RANTES, IP-10, and IFNG (Bio-Rad). Cytokine levels were quantified using the Bioplex-200 system and Bio-Plex 4.0 manager software (Bio-Rad).

Toxicity concentrations. Mean toxic concentration 50 (TC_{50}) values were displayed as the toxic concentration in μg/ml where 50% of the cells remained viable when visualized by trypan blue exclusion (Mediatech, Inc.). Cells treated with sterile DPBS and cell culture media alone were used as negative controls. TC_{50} values for each time point were calculated manually using the Reed and Muench method [41].

Statistical Analysis and Graphs

Statistical analyses and graphical representations were completed and produced, respectively, using Prism software (v4.0; GraphPad, San Diego, CA). One-tailed *t*-tests were employed. A P-value of <0.05 was considered to be statistically significant.

RESULTS

Three-Dimensional Vaginal EC Model Development and Ultrastructural Morphology

Human vaginal ECs cultured in the RWV bioreactor under low fluid-shear conditions exhibited ultrastructural morphology consistent with mammalian vaginal tissue. The 3-D vaginal EC model progressively developed through two stages, early development and late development, each with its own distinct surface morphology. After 19–21 days in the rotating culture, SEM revealed microcarrier bead aggregates covered with a single monolayer of vaginal ECs (early development). This monolayer had surface characteristics remarkably similar to the early vaginal canal and fornix development (Days 2–7) of postnatal BALB/c mice examined by SEM [42, 43]. Vaginal ECs observed at this time point were of variable size and presented a convex apical cell shape covered with sparsely distributed microvilli (Fig. 1, A and C). After approximately 20 additional days in the rotating culture (Days 39–42), 3-D vaginal EC aggregates demonstrated surface morphology of a fully polarized and differentiated vaginal epithelium (late development) (Fig. 1, B and D). Surface characteristics included flattened cell layers of connecting, polygonal apical ECs (typical of a stratified squamous epithelial tissue), densely packed lawns of microvilli of various lengths, vaginal microfolds (i.e., rugae), as well as numerous microridges and secretory vesicles/mucus deposits between adjacent cells and on the apical cell surface (Fig. 2, A, C, E, and G). Representative SEM images of human vaginal tissue displaying these ultrastructural features (i.e., flattened polygonal apical ECs, microfolds, and microridges) are provided in Supplemental Figure S1 (available online at www.biolreprod.org). Collectively, these characteristics of this 3-D vaginal EC model correspond to surface features observed by SEM in the late vaginal canal and fornix development (Days 21–78) of postnatal BALB/c mice, human neovaginal tissue created for females with Mayer-Rokitansky-Kuster-Hauser syndrome, and, most notably, normal human vaginal tissue (Supplemental Figure S1) [5–7, 42, 43].

In addition to examining the surface morphology of our 3-D vaginal EC model, TEM was performed on ultrathin sections in order to visualize the internal ultrastructural features of this model. Internal secretory vesicles were observed primarily in cells on the apical cell surface, suggesting these cells are directly involved in mucus secretion (Fig. 2B). Long,

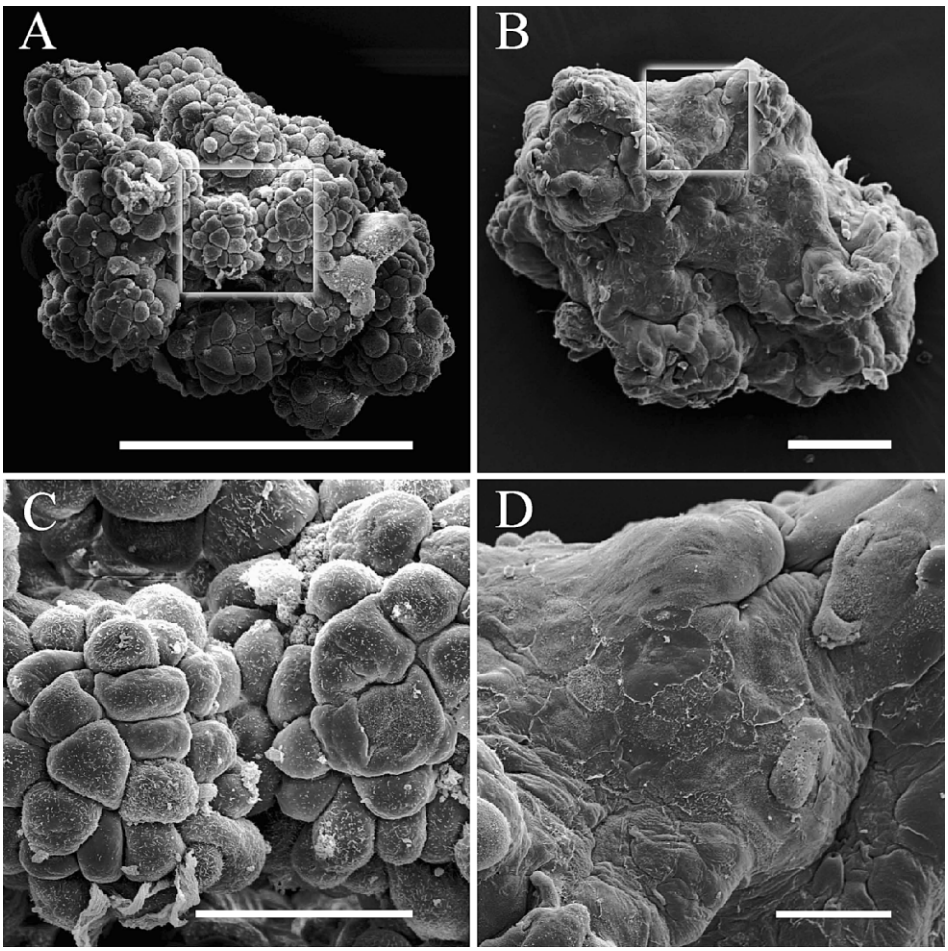

FIG. 1. Scanning electron microscopy of early and late development of 3-D organotypic vaginal epithelial cell (EC) model. **A**) Low magnification SEM of early development (Days 19–21) displaying single layer of vaginal EC. **B**) Low magnification SEM of late development (Days 39–42) displaying multiple, flattened cell layers typical of stratified squamous epithelia. **C**) High magnification image from **A** (boxed area). **D**) High magnification image from **B** (boxed area). Bars = 200 μm (**A** and **B**) and 50 μm (**C** and **D**).

protruding microvilli were also observed primarily on the apical cell surface of the 3-D model; however, short residual microvilli, also referred to as cytoplasmic processes, were observed between adjacent cells near both the apical and the basolateral surfaces (Fig. 2, F and H) [44]. Cellular junctions were also observed throughout the 3-D model tissue (Fig. 2D). In contrast, neither SEM nor TEM revealed long, protruding microvilli or microfolds on the apical surface of confluent vaginal ECs grown on transwell filters, which was verified by observing a significant increase in transepithelial electrical resistance (data not shown). All of these ultrastructural features are remarkably similar to and have been previously reported in SEM and/or TEM from in vivo dissections of mammalian vaginal tissue (e.g., mouse, rabbit, rhesus monkey, and human) [7, 42–46].

Mucin Proteins, Junctional Markers, and Surface Antigen Expression in 3-D Vaginal EC Model Compared to 2-D Monolayers

The expression and cellular localization of several important proteins were investigated by immunofluorescence. One important family of proteins in the female reproductive tract is the mucin (MUC) glycoprotein family. MUC1 is a transmembrane glycoprotein that exhibits both adhesive and antiadhesive properties, effectively creating a barrier against invading microbes at epithelial cell surfaces [47, 48]. MUC1 is also the most widely distributed mucin amongst various human mucosal tissues, including the female reproductive tract, and has been previously reported to be the highest expressed mucin in vaginal epithelial tissue [4, 47–50]. Anti-MUC1 staining displayed intense fluorescence throughout the 3-D vaginal EC model, especially in the crevices and folds of the tissue (Fig. 3A). This has previously been reported to be a region rich in mucin-like glycoproteins in stratified squamous epithelia [50]. The fluorescence intensity of this glycoprotein was lower in 2-D monolayers and its localization was cytoplasmically diffuse (Fig. 3D). In addition to MUC1, the mucin glycoprotein MUC4 (which can be membrane-bound or in a soluble form) is the only other mucin that has been shown to be expressed in the human vaginal epithelium [49, 51]. MUC4 was expressed, albeit at low levels, in the 3-D vaginal EC model while no specific expression was detected in 2-D monolayers (Fig. 3, B and E, respectively). The expression of these two mucin proteins corresponds to previously published data detailing the tissue-specific mucin expression profiles of the female reproductive tract [4, 47, 49–51]. MUC5AC has previously been reported to be highly expressed in human endocervical tissue, but not in ectocervical or vaginal ECs [49]. MUC5AC expression was analyzed as a negative control and was determined to be negative in both the 3-D vaginal EC model and in 2-D monolayers (Fig. 3, C and F, respectively).

The expression and localization of the following two junctional markers were also examined to determine differentiation of the 3-D vaginal EC model: the zona occludens protein, TJP1 (ZO-1), and the adhesive extracellular matrix constituent, E-cadherin (epithelial designation; member of the cadherin superfamily). These proteins are important adhesion molecules necessary for development of intercellular junctional complexes and maintenance of epithelial integrity [52, 53]. E-

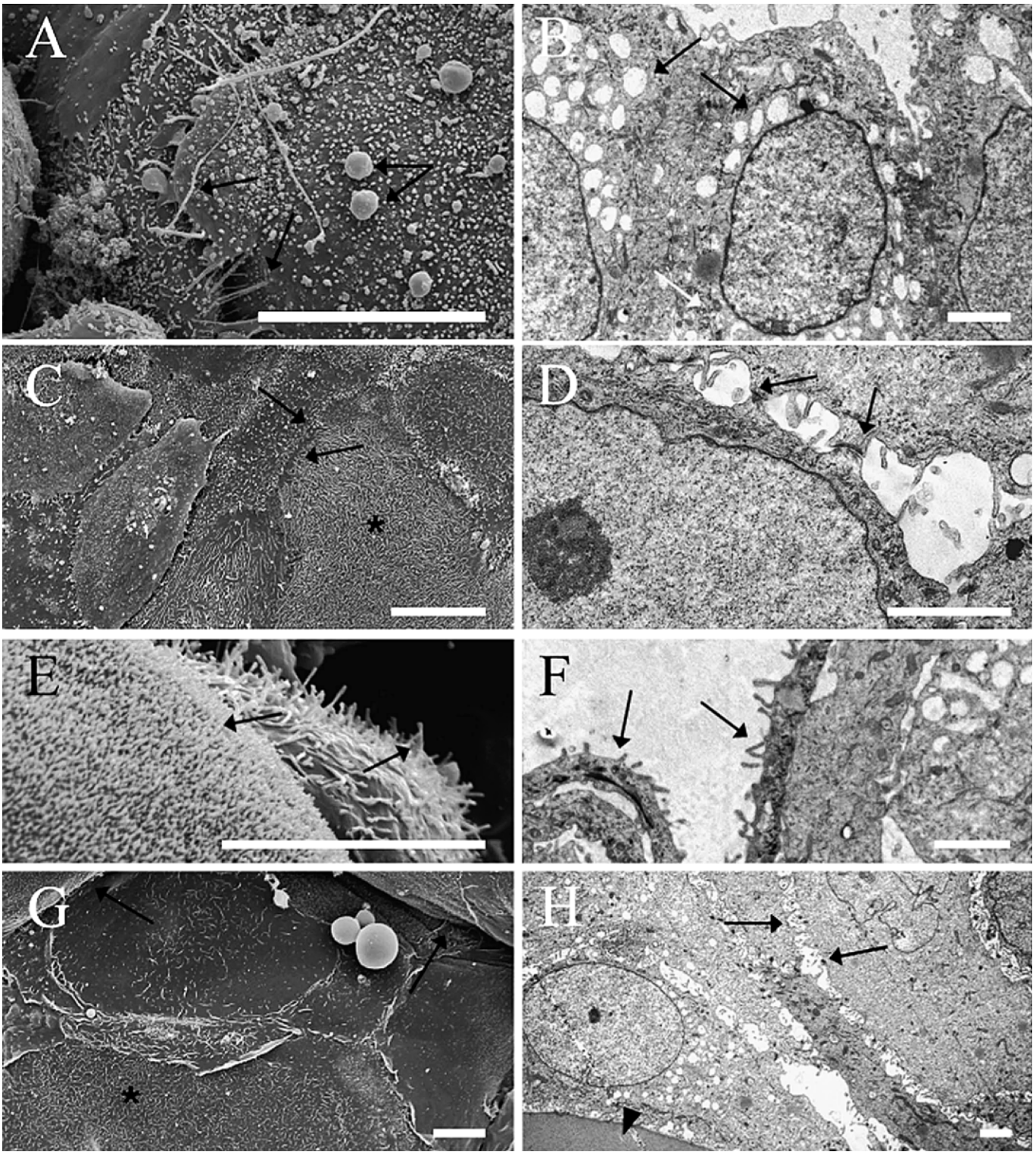

FIG. 2. Scanning electron microscopy (left panel) and transmission electron microscopy (right panel) of physiologically relevant ultrastructural features observed in 3-D organotypic vaginal epithelial cell (EC) model. Arrows indicate extracellular mucus vesicles and string-like secretions (**A**), intracellular secretory vesicles (**B**), tightly adjoining cells on apical surface (**C**), internal cells with prominent hemidesmosomes (**D**), short, stubby, and long protruding microvilli on adjacent cells (**E**), microvilli on apical cell surface (**F**), microfolds (i.e., rugae) (**G**), and intercellular space with residual microvilli (or cytoplasmic processes) (**H**). Asterisks in **C** and **G** indicate cells densely covered with microridges. Arrowhead in **H** indicates microcarrier bead. Bars = 20 μm (**A**, **C**, **E**, **G**) and 2 μm (**B**, **D**, **F**, **H**).

Cadherin and TJP1 were expressed at lower levels in the 2-D monolayers, and immunolocalization revealed the proteins were cytoplasmically diffuse and were not primarily localized to the plasma membrane as in differentiated tissues (Fig. 4, F and G). In contrast, both TJP1 and E-cadherin were highly expressed in the 3-D vaginal EC aggregates and exhibited a honeycomb pattern typical of fully differentiated epithelial cells (Fig. 4, A and B) [52, 53].

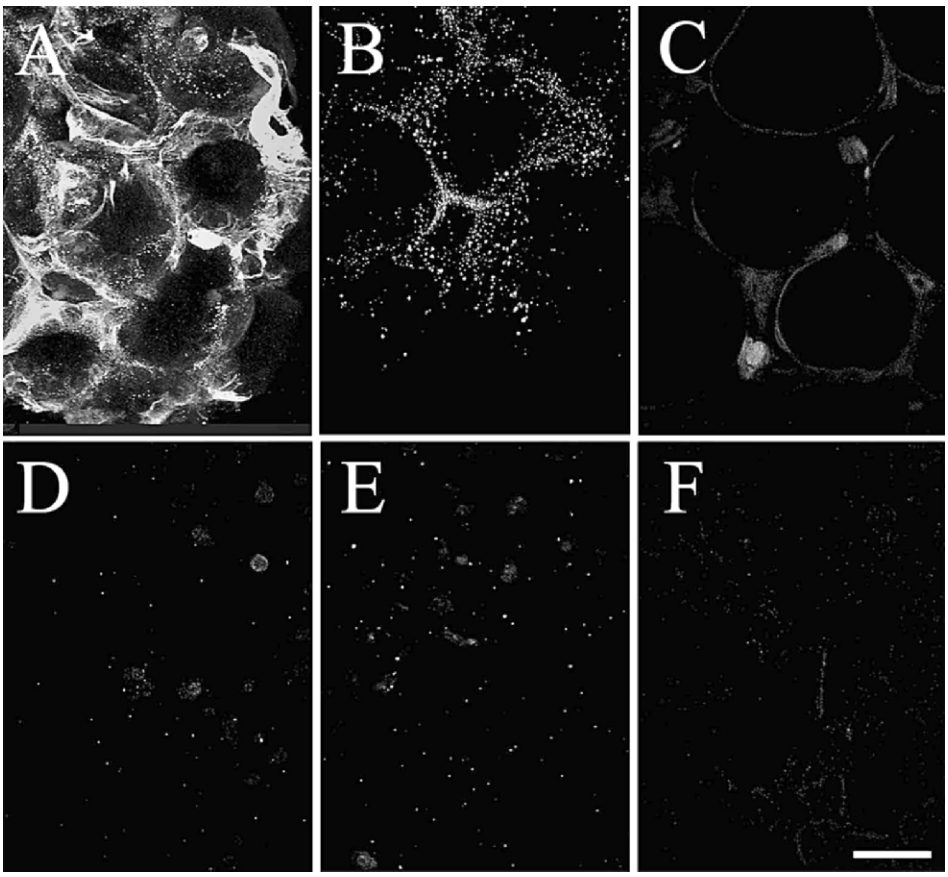

FIG. 3. Mucin production is highly localized and specific in the 3-D vaginal EC model. Immunofluorescence of mucin glycoproteins imaged by laser scanning confocal microscopy. Z-Stacks were reconstructed (optical sections: 1–2 μm, 50–100 sections) demonstrating protein expression levels and localization patterns in the 3-D organotypic vaginal EC model (top panel) compared to confluent monolayer cultures of the same cell line (bottom panel). MUC1 (**A**, **D**), MUC4 (**B**, **E**), and MUC5AC (**C**, **F**). Bar = 100 μm.

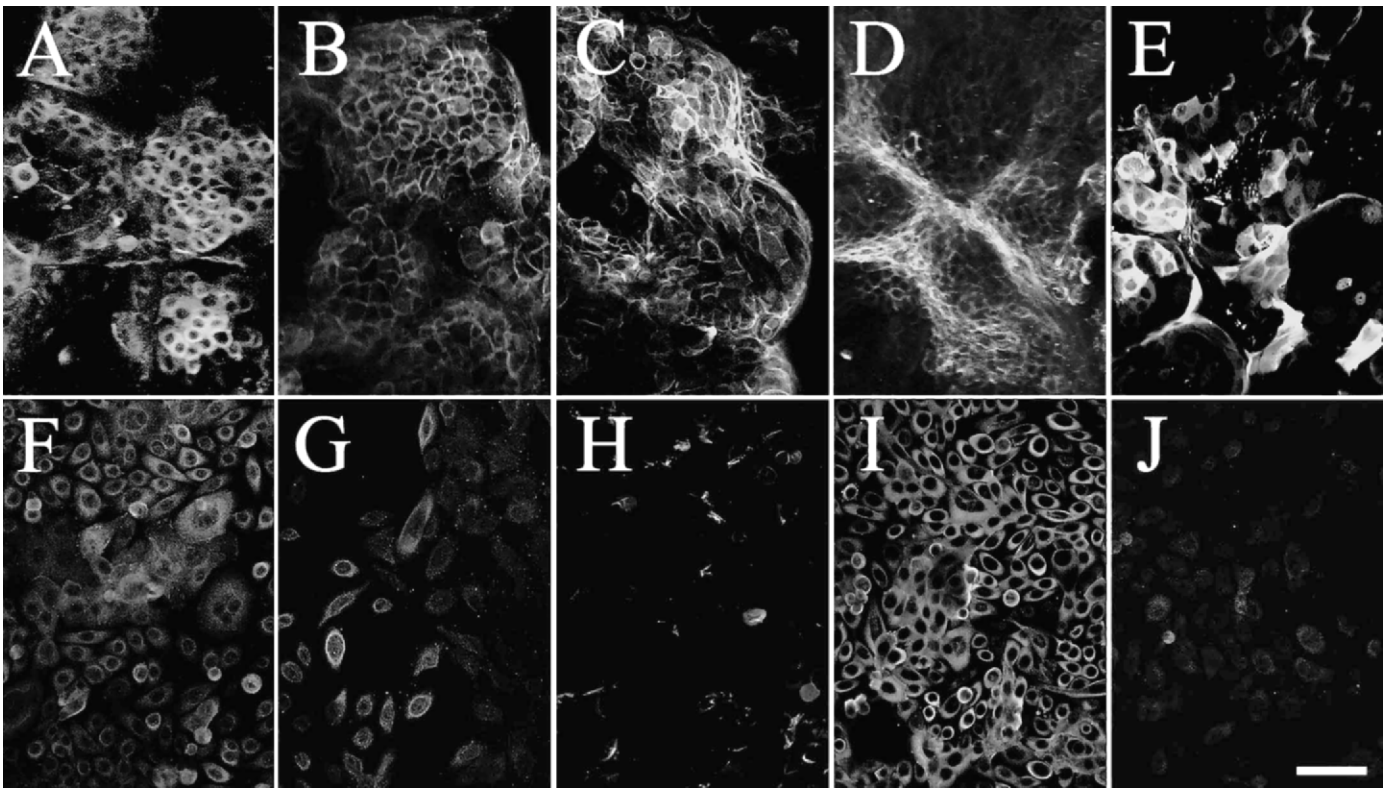

FIG. 4. The 3-D vaginal aggregates demonstrate more specific staining of junctional differentiation and protein markers compared to monolayer counterparts. Immunofluorescence (optical sections: 1–2 μm, 50–100 sections) of markers were imaged by laser scanning confocal microscopy, demonstrating protein expression levels and localization patterns in the 3-D organotypic vaginal EC model (top panel) compared to confluent monolayer cultures of the same cell line (bottom panel). TJP1 (**A**, **F**), E-cadherin (**B**, **G**), ESA (**C**, **H**), CD1D (**D**, **I**), and involucrin (**E**, **J**). Bar = 100 μm.

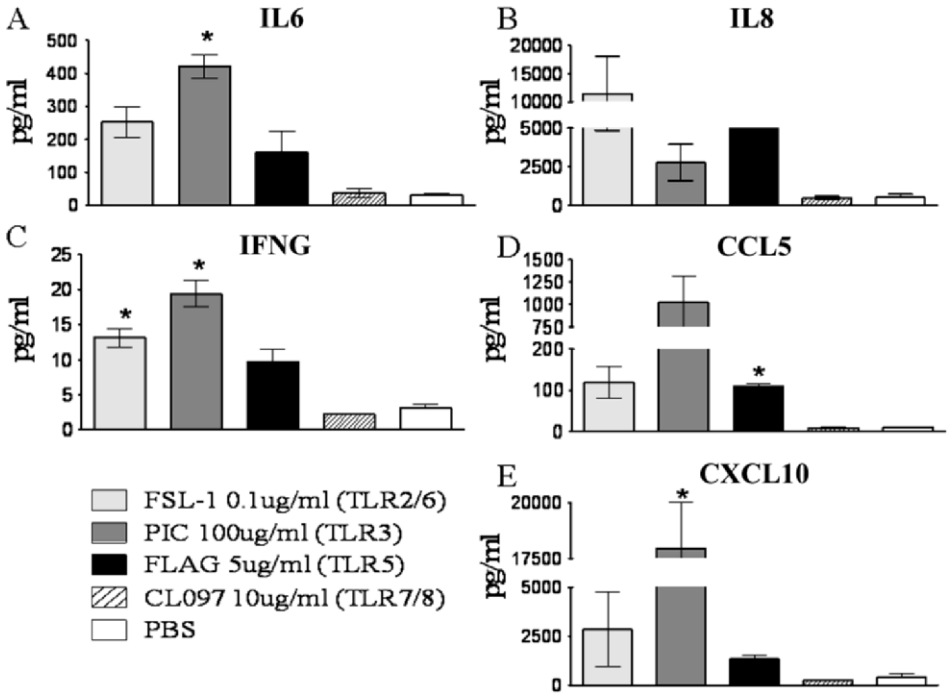

FIG. 5. Cytokine production in response to toll-like receptor (TLR) agonist stimulation in the 3-D vaginal EC model. Cytokines were quantified by cytometric bead array 24 h poststimulation of 3-D organotypic vaginal EC aggregates with FSL-1, PIC, FLAG, and CL097. IL6 (**A**), IL8 (**B**), IFNG (**C**), CCL5 (RANTES; **D**), and CXCL10 (IP-10; **E**). $*P < 0.05$; one-tailed *t*-test compared to the PBS group. Error bars show the standard error of the mean.

Finally, the expression and localization of the glycoproteins epithelial-specific antigen (ESA), CD1D, and the terminal differentiation marker, involucrin, were examined by immunofluorescence. ESA is a basolateral marker of most human epithelia and has been implicated in cell-cell adhesion processes [54, 55]. CD1D is a major histocompatibility complex-like glycoprotein that mediates the presentation of lipid and glycolipid antigens to natural killer T cells [56]. Kawana et al. have recently reported the robust expression of CD1D in both vaginal and ectocervical tissues within the female reproductive tract, but only low-level expression in endocervical on endometrial tissues [56]. Lastly, involucrin, a terminal differentiation marker of keratinocytes, has been shown by Fichorova et al. to be expressed in subpopulations of immortalized vaginal EC monolayers and on the surface of vaginal tissue [3]. Vaginal EC monolayers expressed little to no ESA or involucrin, but displayed positive expression for CD1D (Fig. 4, H–J). Expression of ESA was identified throughout the 3-D vaginal EC layers, while involucrin and CD1D were both primarily localized to the cell surface (Fig. 4, C–E).

TLR Activity

Previously, we have shown that both primary and immortalized vaginal ECs express TLRs 1–6 at the highest levels as profiled by quantitative PCR and are highly responsive to agonists directed against TLRs 2, 3, 5, and 6 [1]. In addition, these studies have indicated that TLRs 7 and 8 are minimally expressed and are not consistently bioactive in vaginal ECs. In order to verify that TLRs 2, 3, 5, and 6 remained functionally responsive in our 3-D vaginal EC model and that there were no profound changes in TLR expression during 3-D development, vaginal cell aggregates were treated with TLR agonists (FSL-1, PIC, FLAG, and CL097). Cytokines IL6 and IFNG, the chemokines IL8 and CXCL10 (IP-10), and CCL5 (RANTES) were quantified by CBA and were found to be increased in concentration in the cell culture medium when cells were treated with FSL-1 (TLR2/6 agonist), PIC (TLR3 agonist), or FLAG (TLR5 agonist) (Fig. 5). Conversely, treatment with CL097, a TLR 7/8 agonist, did not result in cytokine or chemokine levels higher than DPBS controls. These results indicate that the 3-D vaginal EC model retained TLR expression similar to primary and immortalized vaginal monolayers cells and that these TLRs retained functional bioactivity when cultured under rotating conditions [1].

Nonoxynol-9 Toxicity and Cytokine Response

In order to examine the utility of our 3-D model as a platform for evaluating microbicide safety and efficacy, both 3-D vaginal EC aggregates and vaginal EC monolayers were treated with N-9 and examined for viability posttreatment (Fig. 6A). TC_{50} levels were determined for 1.5, 4, 8, and 24 h time points using the Reed and Muench calculation method [41]. TC_{50} levels for the vaginal EC monolayers ranged between 9 μg/ml to 21 μg/ml and likewise did not decrease significantly during the times examined (Fig. 6B). These TC_{50} levels for the vaginal EC monolayers correspond to previous results of many various cell lines grown as traditional monolayers or suspension cell cultures [16]. On the contrary, TC_{50} levels for the 3-D vaginal EC model ranged between 225μg/ml to 425μg/ml for the various time points and did not decrease significantly during the times examined (up to 24 h post-N-9 treatment). These results indicate that our 3-D vaginal EC model has a toxicity response to N-9 much more similar to surgical explant models than their monolayer counterparts [16].

In addition to evaluating viability, cell supernatants from both the 3-D vaginal EC model and vaginal EC monolayers were examined for TRAIL and IL1RN production, both of which are biomarkers of cervicovaginal inflammation. The 3-D vaginal EC model produced higher levels of TRAIL and IL1RN after 24 h at all of the N-9 concentrations tested (10–1000 μg/ml) (Fig. 6, C and D). While the cytokine levels between the 3-D vaginal EC model and the 2-D monolayers were not statistically significant, the higher levels expressed in

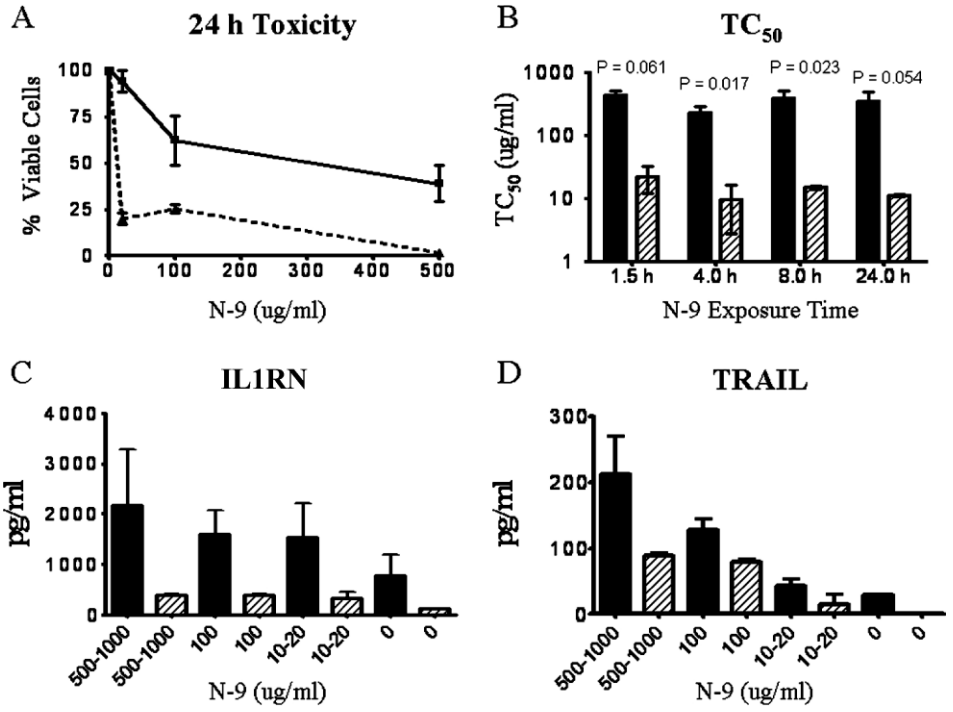

FIG. 6. Validation of the 3-D vaginal EC model for microbicide evaluation. **A**) Nonoxynol-9 dose-dependent viability curve 24 h posttreatment of 3-D organotypic vaginal EC model compared to confluent monolayer cultures of the same cell line. **B**) Nonoxynol-9 TC_{50} levels of 3-D model and confluent monolayers at 1.5, 4, 8, and 24 h posttreatment. TC_{50} levels were calculated from two independent experiments. **C**) Nonoxynol-9 dose-dependant production of cytokine IL1RN 24 h posttreatment of 3-D model compared to confluent monolayers. **D**) Nonoxynol-9 dose-dependent production of cytokine TRAIL 24 h posttreatment of 3-D model compared to confluent monolayers. Solid lines and bars represent the 3-D vaginal EC model, whereas dashed lines and hatched bars represent confluent monolayers of vaginal EC. Error bars show the standard error of the means.

the 3-D vaginal EC model demonstrated a dose-dependent response to N-9 that correlated with the viability results.

DISCUSSION

There is an urgent need for the development of both new microbicide compounds and of new, biologically meaningful platforms in which to evaluate their safety and efficacy [17, 57]. An efficient and high-throughput method for screening candidate microbicides is an essential component of the developmental pipeline. The 3-D vaginal EC model described in this report provides an in vitro platform for microbicide evaluation and STI research that exhibits many of the physiologically relevant features of surgical explants and animal models, but is afforded the high-throughput capabilities of an immortalized human cell line.

Many publications have demonstrated that various types of mammalian cells can only differentiate when cultured under specific cell culture conditions; this concept holds true for human vaginal EC [38, 39, 58]. Although media conditions and growth factor supplements are important factors to consider for any cell culture line or model, additional emphasis can be placed on the extracellular environment in which the cells are grown and on the surface to which they adhere. Transwell filters, extracellular matrix formulations or gels, and the RWV bioreactor have all been used to induce terminal differentiation in a variety of cell types; however, use of the RWV bioreactor technology for tissue culture also mimics the nonstatic growth conditions that proliferating cells are subject to in the human body [38, 39, 58]. Using this RWV technology, we developed and characterized a 3-D vaginal EC model because traditional monolayer cultures have not demonstrated many of the ultrastructural features of human vaginal tissue and the microbicide and the STI communities still rely heavily on tissue explants and animal models for clinical pipeline studies [11, 12].

Morphological analysis of our 3-D vaginal EC model demonstrated a remarkable resemblance to in vivo mammalian tissue, even at the high resolution provided by SEM and TEM analyses. These features included microvilli, tight junctions, microfolds, microridges, and secretory vesicles or mucus. Microfolds are often observed on the surface of cells where a protective layer is advantageous and function by holding mucus in place as well as aid in stabilizing and interlocking the cell layers. Typically these surface elaborations are observed in late proestrus and estrus [45]. The appearance and characterization of microfolds (or rugae) in this 3-D vaginal EC model may provide a particularly important feature for microbicide evaluation and STI research. For example, previous studies have illustrated that several vaginally applied microbicide candidates, tested in *Chlamydia* and herpes simplex virus type 2 (HSV-2) mouse challenge models, failed to penetrate the murine vaginal rugae [27, 59]. This incomplete distribution consequently decreased the compounds' efficacy in vivo, especially when the microbicide and viral/bacterial inoculums were administered independently (i.e., not premixed) [27, 59]. These results indicate that vaginal microfolds may have a substantial impact on the surface distribution of formulated microbicides administered as liquids, foams, gels, etc. This 3-D vaginal EC model offers researchers a high-throughput in vitro method for evaluating the application, distribution, persistence, and protection of vaginally applied microbicide compounds. In addition, this model may provide additional insights into the mechanisms of STI pathogens and their interactions with human vaginal ECs.

The expression and localization of several important junctional and differentiation markers indicated that the 3-D vaginal EC model contained layers of cell-cell junctions important for tissue architecture and integrity, and that these tissue-like aggregates had polarized and differentiated into sheets of stratified squamous epithelia. One additional group of proteins we chose to examine was a subset of the mucin glycoprotein family previously evaluated in the female lower reproductive tract. Gipson et al. [49] have demonstrated by Northern blot and in situ hybridization that human vaginal tissue expresses MUC1 and MUC4, which correlates with our immunofluorescence data. While the exact role of MUC4 in the vaginal cavity is unknown, MUC1 has been implicated as an

extremely important molecule that creates a critical barrier in the female reproductive tract and a variety of other epithelial tissues [47, 48]. The increased immunofluorescence of MUC1 in our 3-D vaginal EC model compared to monolayers of the same cell line indicates our model may possess adhesive and nonadhesive cell surface properties that could greatly influence microbicide distribution and host-pathogen interactions. Interestingly, both MUC1 and MUC4 were found to localize primarily in the folds and crevices of our 3-D vaginal EC model; this was also the location where most secretory/mucus vesicles were observed by SEM analysis.

While physical barriers like tight junctions and mucin proteins play an important role in pathogen defense, the innate immune responses of vaginal ECs are fundamental for STI and microbicide research [2]. Such responses, are in part, due to the activation of pattern recognition receptors (PRRs), including the most well-characterized family, the TLRs, expressed by genital ECs and immune cells [1, 9, 10, 22]. These cells are capable of responding to these stimuli by sending signals that activate neighboring cells as well as activate and recruit professional immune cells to the vaginal cavity. Activation of these PRRs induces a broad array of antimicrobial molecules and recruits effector cells that lead to pathogen elimination. Therefore the activation of the innate immune system through PRR agonists is a strategy for both eliminating pathogens and mounting specific and robust responses to antigens. In particular, vaginal delivery of TLR agonists capable of eliciting a pathogen-specific or molecule-specific immune response have shown great promise for STI prevention strategies, particularly with HSV-2 [60–65]. TLRs 2, 3, 5, and 6 have been shown to be highly expressed in immortalized vaginal EC monolayers; we analyzed the 3-D vaginal model for TLR activity and found there was no significant difference in cytokine/chemokine production between this 3-D vaginal EC model and its monolayer counterpart [1]. This result was somewhat anticipated as we did not expect 3-D architecture to greatly influence TLR expression since many suspension cell lines that do not rely on tight cell-cell interactions (e.g., THP-1 cells or U-397) highly express TLRs and are functionally responsive. A recent report showed that the polyanionic class of microbicide compounds could actually interfere with TLR signaling and thus highlights the importance of evaluating TLR-mediated epithelial immune responses following microbicide exposure [10].

Analysis of the microbicide screening capabilities of our 3-D vaginal EC model was performed using N-9 as our microbicidal test agent. Nonoxynol-9 has been extensively studied in vitro and in vivo because of its antiviral activity and subsequent failures in the clinical pipeline [13, 14]. Many studies have indicated that N-9 is toxic to the vaginal epithelium and can inherently damage the plasma membrane of exposed cells; however, the toxic concentration of this compound has been found to vary greatly between surgical explant models and monolayer or suspension cell lines [16, 17]. Beer et al. examined N-9 toxicity in 127 assays from 5 laboratories that included 11 permanent cell lines and 4 primary cell or tissue types (including a cervical explant model); their results indicated that the cervical explant tissue was significantly more resistant to microbicide toxicity than the various cell lines [16]. This report proposed that this difference was due to the 3-D architecture of the explants; our results further support this hypothesis. While our model did not demonstrate TC_{50} levels as high as the explant results at our 1.5 h time point, this exposure time also showed a great deal of interassay variation with the explant tissue described and may suggest additional variability between surgical explants, specifically for short-term exposure studies [16]. When grown in 3-D conditions, our vaginal EC model demonstrated comparable TC_{50} levels to that of cervical explant tissue, especially between 4 and 24 h poststimulation [16].

The significance of this 3-D vaginal epithelial model is the formation of a stratified, squamous epithelium in vitro with cellular proliferation, differentiation, progressive keratinization, and ultimately desquamation of cells that resemble exfoliated cells obtained in vivo. This model, therefore, has the potential to be utilized not only for microbicide screening, but could also be used for STI pathogenesis and/or commensal pathogen studies, to study the effect of exogenous factors such as hormones and growth factors and to better understand the innate immune responses (PAMP recognition, secretion of antimicrobial peptides and defensins, etc.) of this mucosal tissue. In future studies, we believe it will be useful to determine if 3-D vaginal cells are estrogen responsive. In preliminary studies, we have tested a high and low concentration of 17-beta estradiol (within the normally active range of the hormone) and found that there was no significant difference in proliferation, morphology, or cell viability among estrogen-treated versus mock-treated cells. Because of the use of other growth factors in the serum-free medium, however, we cannot make any conclusions related to the cells' estrogen responsiveness until a comprehensive analysis is completed. Our future plans also include utilizing this rotary cell culture method to develop additional 3-D models of female reproductive tract mucosal tissues that could potentially aid in the study of ascending STI pathogens, including *Chlamydia trachomatis* and *Neisseria gonorrhea*. Additionally, we intend to explore the incorporation of various immune cells (i.e., monocytes, macrophages, dendritic cells, etc.) into our 3-D culture models as these coculture models may help delineate the functional role of each cellular constituent that comprises the female reproductive tract when the various tissues are exposed to other STI pathogens (including HIV), chemical compounds, or bioactive molecules.

ACKNOWLEDGMENTS

The authors would like to thank Dr. Richard Pyles for providing the V19I cell line, Daaimah LaVigne and Emily Richter for cell culture assistance, and Dr. Doug Daniel for technical assistance on the confocal microscope. The authors are also grateful to David Lowry and Dr. Robert Roberson for their advice regarding sample preparation for electron microscopy studies as well as their assistance reviewing the electron micrographs. All electron microscopy and preparation was carried out in the Electron Microscopy Laboratory in the School of Life Sciences Bioimaging Facility at Arizona State University. All confocal microscopy was performed in the Center for BioOptical Nanotechnology in the Biodesign Institute at Arizona State University. The authors would also like to acknowledge the kind permission provided by Dr. Hans Ludwig and Springer-Verlag for reproduction of SEM micrographs (included as a Supplemental Figure S1 in this manuscript) from *The Human Female Reproductive Tract: A Scanning Electron Microscopy Altas* [7].

REFERENCES

1. Herbst-Kralovetz MM, Quayle AJ, Ficarra M, Greene S, Rose WA II, Chesson R, Spagnuolo RA, Pyles RB. Quantification and comparison of toll-like receptor expression and responsiveness in primary and immortalized human female lower genital tract epithelia. Am J Reprod Immunol 2008; 59:212–224.
2. Quayle AJ. The innate and early immune response to pathogen challenge in the female genital tract and the pivotal role of epithelial cells. J Reprod Immunol 2002; 57:61–79.
3. Fichorova RN, Rheinwald JG, Anderson DJ. Generation of papillomavirus-immortalized cell lines from normal human ectocervical, endocervical, and vaginal epithelium that maintains expression of tissue-specific differentiation proteins. Biol Reprod 1997; 57:847–855.

4. DeSouza MM, Lagow E, Carson DD. Mucin functions and expression in mammalian reproductive tract tissues. Biochem Biophys Res Comm 1998; 247:1–6.
5. Fedele L, Bianchi S, Berlanda N, Fontana E, Raffaelli R, Bulfoni A, Braidotti P. Neovaginal mucosa after Vecchietti's laparoscopic operation for Rokitansky syndrome: structural and ultrastructural study. Am J Obstet Gynecol 2006; 195:56–61.
6. Barberini F, Vizza E, Montanino M, Marcoccia S, Montanino G. Vaginal reconstruction by skin grafts: a scanning electron microscopic evaluation. Ann Anat 1992; 174:517–522.
7. Ludwig H, Metzger H. The Human Female Reproductive Tract: A Scanning Electron Microscopy Altas. New York: Springer-Verlag; 1976: 8–15.
8. Fichorova RN, Anderson DJ. Differential expression of immunobiological mediators by immortalized human cervical and vaginal epithelial cells. Biol Reprod 1999; 60:508–514.
9. Soboll G, Schaefer TM, Wira CR. Effect of toll-like receptor (TLR) agonists on TLR and microbicide expression in uterine and vaginal tissues of the mouse. Am J Reprod Immunol 2006; 55:434–446.
10. Trifonova RT, Doncel GF, Fichorova RN. Polyanionic microbicides modify TLR-mediated cervicovaginal immune responses. Antimicrob Agents Chemother 2009; 53:1490–1500.
11. Cummins JE Jr, Doncel GF. Biomarkers of cervicovaginal inflammation for the assessment of microbicide safety. Sex Transm Dis 2009; 36:S84–S91.
12. Doncel GF, Chandra N, Fichorova RN. Preclinical assessment of the proinflammatory potential of microbicide candidates. J Acquir Immune Defic Syndr 2004; 37:S174–S180.
13. van de Wijgert JH, Shattock RJ. Vaginal microbicides: moving ahead after an unexpected setback. AIDS 2007; 21:2369–2376.
14. Hiller SL, Moench T, Shattock R, Black R, Reichelderfer P, Veronese F. In vitro and in vivo: the story of nonoxynol 9. J Acquir Immune Defic Syndr 2005; 39:1–8.
15. Ayehunie S, Cannon C, Lamore S, Kubilus J, Anderson DJ, Pudney J, Klausner M. Organotypic human vaginal-ectocervical tissue model for irritation studies of spermicides, microbicides, and feminine-care products. Toxicol In Vitro 2006; 20:689–698.
16. Beer BE, Doncel GF, Krebs FC, Shattock RJ, Fletcher PS, Buckheit RW Jr, Watson K, Dezzutti CS, Cummins JE, Bromley E, Richarson-Harman N, Pallansch LA, et al. In vitro testing of nonoxynol-9 as a potential anti-human immunodeficiency virus microbicide: a retrospective analysis of results from five laboratories. Antimicrob Agents Chemother 2006; 50: 713–723.
17. Krebs FC, Miller SR, Catalone BJ, Fichorova R, Anderson D, Malamud D, Howett MK, Wigdahl B. Comparative in vitro sensitivities of human immune cell lines, vaginal and cervical epithelial cell lines, and primary cells to candidate microbicides nonoxynol 9, C31G, and sodium dodecyl sulfate. Antimicrob Agents Chemother 2002; 46:2292–2298.
18. Squier CA, Mantz MJ, Schlievert PM, Davis CC. Porcine vagina ex vivo as a model for studying permeability and pathogenesis in mucosa. J Pharm Sci 2008; 97:9–21.
19. Fichorova RN. Guiding the vaginal microbicide trials with biomarkers of inflammation. J Acquir Immune Defic Syndr 2004; 37:S184–S193.
20. Fichorova RN, Bajpai M, Chandra N, Hsiu JG, Spangler M, Ratnam V, Doncel GF. Interleukin (IL)-1, IL-6, and IL-8 predict mucosal toxicity of vaginal microbicidal contraceptives. Biol Reprod 2004; 71:761–769.
21. Fichorova RN, Desai PJ, Gibson FC III, Genco CA. Distinct proinflammatory host responses to Neisseria gonorrhoeae infection in immortalized human cervical and vaginal epithelial cells. Infect Immun 2001; 69:5840–5848.
22. Gribar SC, Richardson WM, Sodhi CP, Hackam DJ. No longer an innocent bystander: epithelial toll-like receptor signaling in the development of mucosal inflammation. Mol Med 2008; 14:645–659.
23. Fazeli A, Bruce C, Anumba DO. Characterization of toll-like receptors in the female reproductive tract in humans. Hum Reprod 2005; 20:1372–1378.
24. Pioli PA, Amiel E, Schaefer TM, Connolly JE, Wira CR, Guyre PM. Differential expression of toll-like receptors 2 and 4 in tissues of the human female reproductive tract. Infect Immun 2004; 72:5799–5806.
25. McGowin CL, Ma L, Martin DH, Pyles RB. Mycoplasma genitalium-encoded MG309 activates NF-kappaB via toll-like receptors 2 and 6 to elicit proinflammatory cytokine secretion from human genital epithelial cells. Infect Immun 2009; 77:1175–1181.
26. Milligan GN, Dudley KL, Bourne N, Reece A, Stanberry LR. Entry of inflammatory cells into the mouse vagina following application of candidate microbicides: comparison of detergent-based and sulfated polymer-based agents. Sex Transm Dis 2002; 29:597–605.
27. Achilles SL, Shete PB, Whaley KJ, Moench TR, Cone RA. Microbicide efficacy and toxicity tests in a mouse model for vaginal transmission of Chlamydia trachomatis. Sex Transm Dis 2002; 29:655–664.
28. Patton DL, Cosgrove Sweeney YT, Paul KJ. A summary of preclinical topical microbicide vaginal safety and chlamydial efficacy evaluations in a pigtailed macaque model. Sex Transm Dis 2008; 35:889–897.
29. Nickerson CA, Goodwin TJ, Terlonge J, Ott CM, Buchanan KL, Uicker WC, Emami K, LeBlanc CL, Ramamurthy R, Clarke MS, Vanderburg CR, Hammond T, et al. Three-dimensional tissue assemblies: novel models for the study of Salmonella enterica serovar typhimurium pathogenesis. Infect Immun 2001; 69:7106–7120.
30. Carterson AJ, Höner zu Bentrup K, Ott CM, Clarke MS, Pierson DL, Vanderburg CR, Buchanan KL, Nickerson CA, Schurr MJ. A549 lung epithelial cells grown as three-dimensional aggregates: alternative tissue culture model for Pseudomonas aeruginosa pathogenesis. Infect Immun 2005; 73:1129–1140.
31. Höner zu Bentrup K, Ramamurthy R, Ott CM, Emami K, Nelman-Gonzalez M, Wilson JW, Richter EG, Goodwin TJ, Alexander JS, Pierson DL, Pellis N, Buchanan KL, et al. Three-dimensional organotypic models of human colonic epithelium to study the early stages of enteric salmonellosis. Microbes Infect 2006; 8:1813–1825.
32. LaMarca HL, Ott CM, Höner zu Bentrup K, LeBlanc CL, Pierson DL, Nelson AB, Scandurro AB, Whitley GS, Nickerson CA, Morris CA. Three-dimensional growth of extravillous cytotrophoblasts promotes differentiation and invasion. Placenta 2005; 26:709–720.
33. Myers TA, Nickerson CA, Kaushal D, Ott CM, Höner zu Bentrup K, Ramamurthy R, Nelman-Gonzales M, Pierson DL, Philipp MT. Closing the phenotypic gap between transformed neuronal cell lines in culture and untransformed neurons. J Neurosci Methods 2008; 174:31–41.
34. Nickerson CA, Richter EG, Ott CM. Studying host-pathogen interactions in 3-D: organotypic models for infectious disease and drug development. J Neuroimmune Pharmacol 2007; 2:26–31.
35. Vamvakidou AP, Mondrinos MJ, Petushi SP, Garcia FU, Lelkes PI, Tozeren A. Heterogeneous breast tumoroids: an in vitro assay for investigating cellular heterogeneity and drug delivery. J Biomol Screen 2007; 12:13–20.
36. Pound JC, Green DW, Roach HI, Mann S, Oreffo RO. An ex vivo model for chondrogenesis and osteogenesis. Biomaterials 2007; 28:2839–2849.
37. Webb MA, Platton SL, Dennison AR, James RF. Immunohistochemical evidence that culture in the high aspect rotating vessel can up-regulate hormone expression in growth dedifferentiated PHHI-derived islet cells. In Vitro Cell Dev Biol Anim 2007; 43:210–214.
38. Unsworth BR, Lelkes PI. Growing tissues in microgravity. Nat Med 1998; 4:901–907.
39. Navran S. The application of low shear modeled microgravity to 3-D cell biology and tissue engineering. Biotechnol Ann Rev 2008; 14:275–296.
40. McGowin CL, Popov VL, Pyles RB. Intracellular Mycoplasma genitalium infection of human vaginal and cervical epithelial cells elicits distinct patterns of inflammatory cytokine secretion and provides a possible survival niche against macrophage-mediated killing. BMC Microbiol 2009; 9:139.
41. Reed LJ, Muench H. A simple method of estimating fifty per cent endpoints. Am J Hyg 1938; 27:493–497.
42. Plapinger L. Surface morphology of uterine and vaginal epithelia in mice during normal postnatal development. Biol Reprod 1982; 26:961–972.
43. Plapinger L. Morphological effects of diethylstilbestrol on neonatal mouse uterus and vagina. Cancer Res 1981; 41:4667–4677.
44. Takasugi N, Kamishima Y. Development of vaginal epithelium showing irreversible proliferation and cornification in neonatally estrogenized mice: an electron microscope study. Dev Growth Differ 1973; 15:127–140.
45. Barberini F, Correr S, De Santis F, Motta PM. The epithelium of the rabbit vagina: a microtopographical study by light, transmission and scanning electron microscopy. Arch Histol Cytol 1991; 54:365–378.
46. King BF. Ultrastructure of the nonhuman primate vaginal mucosa: epithelial changes during the menstrual cycle and pregnancy. J Ultrastruct Res 1983; 82:1–18.
47. DeSouza MM, Surveyor GA, Price RE, Juilan J, Kardon R, Zhou X, Gendler S, Hilkens J, Carson DD. MUC1/episialin: a critical barrier in the female reproductive tract. J Reprod Immunol 1999; 45:127–158.
48. McAuley JL, Linden SK, Png CW, King RM, Pennington HL, Gendler SJ, Florin TH, Hill GR, Korolik V, McGuckin MA. MUC1 cell surface mucin is a critical element of the mucosal barrier to infection. J Clin Invest 2007; 117:2313–2324.
49. Gipson IK, Ho SB, Spurr-Michaud SJ, Tisdale AS, Zhan Q, Torlakovic E, Pudney J, Anderson DJ, Toribara NW, Hill JA III. Mucin genes expressed by human female reproductive tract epithelia. Biol Reprod 1997; 56:999–1011.

50. Gipson IK, Spurr-Michaud SJ, Tisdale AS, Kublin C, Cintron C, Keutmann H. Stratified squamous epithelia produce mucin-like glycoproteins. Tissue Cell 1995; 27:397–404.
51. Idris N, Carraway KL. Sialomucin complex (Muc4) expression in the rat female reproductive tract. Biol Reprod 1999; 61:1431–1438.
52. Langbein L, Grund C, Kuhn C, Praetzel S, Kartenbeck J, Brandner JM, Moll I, Franke WW. Tight junctions and compositionally related junctional structures in mammalian stratified epithelia and cell cultures derived therefrom. Eur J Cell Biol 2002; 81:419–435.
53. Maretzky T, Reiss K, Ludwig A, Buchholz J, Scholz F, Proksch E, de Strooper B, Hartmann D, Saftig P. ADAM10 mediates E-cadherin shedding and regulates epithelial cell-cell adhesion, migration, and β-catenin translocation. Proc Natl Acad Sci U S A 2005; 102:9182–9187.
54. Schmeichel KL, Bissell MJ. Modeling tissue-specific signaling and organ function in three dimensions. J Cell Sci 2003; 116:2377–2388.
55. Litvinov SV, Velders MP, Bakker HA, Fleuren GJ, Warnaar SO. Ep-CAM: a human epithelial antigen is a homophilic cell-cell adhesion molecule. J Cell Biol 1994; 125:437–446.
56. Kawana K, Matsumoto J, Miura S, Shen L, Kawana Y, Nagamatsu T, Yasugi T, Fujii T, Yang H, Quayle AJ, Taketani Y, Schust DJ. Expression of CD1d and ligand-induced cytokine production are tissue specific in mucosal epithelia of the human lower reproductive tract. Infect Immun 2008; 76:3011–3018.
57. Mauck CK. Biomarkers for evaluating vaginal microbicides and contraceptives: discovery and early validation. Sex Transm Dis 2009; 36:S73–S75.
58. Hammond TG, Hammond JM. Optimized suspension culture: the rotating-wall vessel. Am J Physiol Renal Physiol 2001; 281:F12–F25.
59. Cone RA, Hoen T, Wong X, Abusuwwa R, Anderson DJ, Moench TR. Vaginal microbicides: detecting toxicities in vivo that paradoxically increase pathogen transmission. BMC Infect Dis 2006; 6:90.
60. Herbst-Kralovetz MM, Pyles RB. Quantification of poly(I:C)-mediated protection against genital herpes simplex virus type 2 infection. J Virol 2006; 80:9988–9997.
61. Herbst MM, Pyles RB. Immunostimulatory CpG treatment for genital HSV-2 infections. J Antimicrob Chemother 2003; 52:887–889.
62. Herbst-Kralovetz M, Pyles R. Toll-like receptors, innate immunity and HSV pathogenesis. Herpes 2006; 13:37–41.
63. Harandi AM, Eriksson K, Holmgren J. A protective role of locally administered immunostimulatory CpG oligodeoxynucleotide in a mouse model of genital herpes infection. J Virol 2003; 77:953–962.
64. Pyles RB, Higgins D, Chalk C, Zalar A, Eiden J, Brown C, Van Nest G, Stanberry LR. Use of immunostimulatory sequence-containing oligonucleotides as topical therapy for genital herpes simplex virus type 2 infection. J Virol 2002; 22:11387–11396.
65. McCluskie MJ, Cartier JL, Patrick AJ, Sajic D, Weeratna RD, Rosenthal KL, Davis HL. Treatment of intravaginal HSV-2 infection in mice: a comparison of CpG oligodeoxynucleotides and resiquimod (R-848). Antiviral Res 2006; 69:77–85.

Downloaded from www.biolreprod.org